



# FAM83H and Autosomal Dominant Hypocalcified Amelogenesis Imperfecta

Journal of Dental Research  
2021, Vol. 100(3) 293–301  
© International & American Associations  
for Dental Research 2020  
Article reuse guidelines:  
sagepub.com/journals-permissions  
DOI: 10.1177/0022034520962731  
journals.sagepub.com/home/jdr

S.K. Wang<sup>1,2</sup>, H. Zhang<sup>1</sup>, C.Y. Hu<sup>3</sup>, J.F. Liu<sup>4</sup>, S. Chadha<sup>1</sup>, J.W. Kim<sup>5,6</sup> ,  
J.P. Simmer<sup>1</sup> , and J.C.C. Hu<sup>1</sup>

## Abstract

Autosomal dominant hypocalcified amelogenesis imperfecta (ADHCAI; OMIM # 130900) is a genetic disorder exhibiting severe hardness defects and reduced fracture toughness of dental enamel. While the condition is nonsyndromic, it can be associated with other craniofacial anomalies, such as malocclusions and delayed or failed tooth eruption. Truncation mutations in *FAM83H* (OMIM \*611927) are hitherto the sole cause of ADHCAI. With human genetic studies, *Fam83h* knockout and mutation–knock-in mouse models indicated that *FAM83H* does not serve a critical physiologic function during enamel formation and suggested a neomorphic mutation mechanism causing ADHCAI. The function of *FAM83H* remains obscure. *FAM83H* has been shown to interact with various isoforms of casein kinase I (CKI) and keratins and to mediate organization of keratin cytoskeletons and desmosomes. By considering *FAM83H* a scaffold protein to anchor CKIs, further molecular characterization of the protein could gain insight into its functions. In this study, we characterized 9 kindreds with ADHCAI and identified 3 novel *FAM83H* truncation mutations: p.His437\*, p.Gln459\*, and p.Glu610\*. Some affected individuals exhibited hypoplastic phenotypes, in addition to the characteristic hypocalcification enamel defects, which have never been well documented. Failed eruption of canines or second molars in affected persons was observed in 4 of the families. The p.Glu610\* mutation was located in a gap area (amino acids 470 to 625) within the zone of previously reported pathogenic variants (amino acids 287 to 694). In vitro pull-down studies with overexpressed *FAM83H* proteins in HEK293 cells demonstrated an interaction between *FAM83H* and *SEC16A*, a protein component of the COP II complex at endoplasmic reticulum exit sites. The interaction was mediated by the middle part (amino acids 287 to 657) of mouse *FAM83H* protein. Results of this study significantly extended the phenotypic and genotypic spectrums of *FAM83H*-associated ADHCAI and suggested a role for *FAM83H* in endoplasmic reticulum–to–Golgi vesicle trafficking and protein secretion (dbGaP phs001491.v1.p1).

**Keywords:** tooth eruption, hypodontia, *SEC16A*, CKI, dental enamel, mutation

## Introduction

Amelogenesis imperfecta (AI) is a diagnostic term for nonsyndromic genetic disorders primarily affecting dental enamel (Witkop and Sauk 1976; Witkop 1988). “AI” is also used to indicate the presence of an enamel phenotype in syndromes. Three main AI phenotypes are generically categorized to delineate the spectrum of enamel defects: hypoplastic, hypomaturation, and hypocalcified (Hu et al. 2007). While hypoplastic AI describes a reduced thickness of dental enamel, hypomaturation refers to an enamel hardness defect. Hypocalcified AI specifies a distinct morphologic form of enamel malformations with markedly soft consistency and frequent dull brown discoloration. While hypocalcified enamel is subjected to fracture, it is generally of normal thickness. Mutational analyses on AI kindreds have established a substantial causality between autosomal dominant hypocalcified AI (ADHCAI) and *FAM83H* (family with sequence similarity 83 member H, OMIM \*611927) truncation mutations (Kim et al. 2008; Lee et al. 2008). All 32 disease-causing *FAM83H* mutations reported to date are either nonsense mutations or frameshifts that truncate the original 1,179–amino acid *FAM83H* protein (Appendix Table). Specifically, only mutations that terminate the protein between 287 and 694 amino acids have been reported to be

pathogenic. A mouse model carrying a truncation *FAM83H* mutation recently demonstrated that mutant *FAM83H* proteins are required to disturb amelogenesis and cause enamel defects (Wang et al. 2019).

As the primary structure of *FAM83H* protein provides little information about its function, efforts have been made for its

<sup>1</sup>Department of Biologic and Materials Sciences, School of Dentistry, University of Michigan, Ann Arbor, MI, USA

<sup>2</sup>Department of Dentistry, School of Dentistry, National Taiwan University, Jhongheng District, Taipei City, Taiwan

<sup>3</sup>Department of Prosthodontics, National Taiwan University Hospital, Jhongheng District, Taipei City, Taiwan

<sup>4</sup>Division of Pediatric Dentistry, Department of Stomatology, Taichung Veterans General Hospital, Xitun District, Taichung City, Taiwan

<sup>5</sup>Department of Pediatric Dentistry and Dental Research Institute, School of Dentistry, Seoul National University, Seoul, Republic of Korea

<sup>6</sup>Department of Molecular Genetics and Dental Research Institute, School of Dentistry, Seoul National University, Seoul, Republic of Korea

A supplemental appendix to this article is available online.

## Corresponding Author:

S.K. Wang, Department of Dentistry, School of Dentistry, National Taiwan University, No. 1, Changde St., Jhongheng District, Taipei City 100, Taiwan.  
Email: shihkaiw@umich.edu; shihkaiw@ntu.edu.tw

molecular characterization. Several groups have demonstrated that FAM83H interacts with different isoforms of CK1 (casein kinase 1) through its N-terminal domain and proposed a role for FAM83H to properly anchor CK1s to their subcellular localizations (Kuga, Kume, et al. 2016; Fulcher et al. 2018). In particular, FAM83H was shown to recruit CK1 to keratin filaments (Kuga, Kume, et al. 2016) and mediate organization of keratin cytoskeleton (Kuga et al. 2013). It was also suggested that ADHCAI-associated *FAM83H* mutations cause keratin disorganization and disruption of desmosomes in ameloblasts (Kuga, Sasaki, et al. 2016). Nevertheless, despite all these findings, the functions of FAM83H remain far from fully understood. We previously investigated the interactome of the mouse FAM83H protein using affinity purification combined with mass spectrometry and identified many potential FAM83H interacting proteins (Wang et al. 2015). Full delineation of these protein-protein interactions will unravel the molecular and cellular functions of FAM83H. In this study, we describe 9 families with ADHCAI and report 3 novel *FAM83H* disease-causing mutations, which extend phenotypic and genotypic spectrums of the disease. With in vitro experiments, we demonstrate an interaction between FAM83H and SEC16A, a protein component in the COP II complex important for vesicular trafficking from the endoplasmic reticulum (ER) to the Golgi (Duden 2003; Blackburn et al. 2019), suggesting a role for FAM83H in intracellular vesicle trafficking.

## Materials and Methods

### Recruitment of Families with ADHCAI

The human study protocol and consent forms were reviewed and approved by the Institutional Review Board Committees at the National Taiwan University Hospital and the University of Michigan. Following comprehensive explanation and discussion of study contents, all participants signed written consents. Phenotypic characterization and pedigree construction were conducted through history taking and clinical and radiographic examinations. Blood or saliva samples were collected for mutational analyses. All of the aforementioned procedures were specified in the study protocols and followed the Declaration of Helsinki.

### Mutational Analyses

The genomic DNA of each participant was extracted from a sample of 5 mL of peripheral blood or 2 mL of nonstimulated saliva. For families 2, 3, 4, and 6, whole exome sequencing and analysis were conducted following a previously published protocol (Zhang et al. 2019) to search for disease-causing mutations. The sequencing procedures and bioinformatic analyses were previously described (Kim et al. 2019). For families 1, 5, 7, and 8, a target gene approach was employed to identify *FAM83H* truncation mutations. The 5' coding region of *FAM83H* Exon5 was amplified with 4 pairs of primers. The amplicons were then sequenced by Sanger sequencing. Sequence variants were called by comparing the resulting

sequencing data with human reference sequence and annotated with NM\_198488.3 and NG\_016652.1 for numbering cDNA and gDNA positions, respectively.

### Expression Constructs, Cell Culture, and Plasmid Transfection

Four constructs to overexpress mouse FAM83H with different lengths were generated as previously described. Three respective premature stop codons were introduced into the pCMV-Tag2B-*Fam83h* construct (encoding full-length 1,209 amino acids) to express 3 truncated FAM83H proteins (1 to 287, 1 to 657, and 1 to 697 amino acids). All encoded FAM83H proteins contained an N-terminal Flag tag. The construct expressing Halo-tagged human SEC16A (FHC00048) and the HaloTag control vector (G6591) were purchased from Promega Corporation. For transient plasmid transfection, human HEK293 cells were prepared to reach the confluency of 75% to 80%. Plasmid (4 µg) in 10 µL of Lipofectamine 2000 (Life Technologies) was diluted with 500 µL of Opti-MEM reduced-serum medium (Life Technologies) and added to the culture media. After 6-h incubation, the culture media was changed to DMEM, and the cells were cultured for 42 h before harvest.

### Pull-down Assays, SDS-PAGE, and Immunoblotting

Dynabeads Protein A Immunoprecipitation Kit (Life Technologies) with Anti-Flag antibody (F7425; Sigma-Aldrich) was used for pull-down experiments per the manufacturers' instructions. The immunoprecipitates, with cell lysates, were then run through SDS-PAGE and analyzed with immunoblotting. Primary antibodies used for immunoblotting included anti-Flag (F7425; Sigma-Aldrich), anti-SEC16A (ab70722; Abcam), and anti-HaloTag (G9211; Promega Corporation). Two secondary antibodies were used: ECL anti-rabbit IgG (NA934V; GE Healthcare) and anti-mouse IgG+IgM HRP (ab47827; Abcam).

## Results

### Novel *FAM83H* Mutations Causing ADHCAI

We identified and characterized 8 new families with ADHCAI caused by 7 *FAM83H* mutations, 3 of which have never been reported. All mutations were nonsense mutations located in the last exon of the *FAM83H* gene. All affected individuals carried a heterozygous *FAM83H* truncation mutation within the critical segment of Ser<sup>287</sup> to Glu<sup>694</sup> that segregated with the presence of enamel defects in each family.

### Family 1 and Family 2 (c.1309\_1311delinsTAA; p.His437\*)

Families 1 and 2 were from Taiwan and apparently unrelated. The proband of family 1 (IV:2; age, 16 y) inherited enamel defects from her father (Fig. 1A–D). Her enamel had mostly

chipped off, exposing dentin and leading to dark brown discolorations. Radiographically, all permanent teeth were present. Tooth number 31 had completed root formation but failed to erupt, without apparent pericoronal pathology. While all erupted tooth crowns showed a moth-eaten appearance with enamel remaining only in cervical areas, the unerupted teeth exhibited a full thickness of enamel that contrasted little with dentin, indicating hypocalcification.

The proband of family 2 (II:2; age, 13 y) had an enamel phenotype similar to that of the family 1 proband, although the enamel chipping and tooth discoloration were less severe and all teeth had erupted (Fig. 1E–H). Some normal-looking enamel could be found on the cusp tips of bicuspids and distal lingual cusp of mandibular second molars.

A novel heterozygous *FAM83H* truncation mutation, NG\_016652.1: g.10593\_10595delins TAA; NM\_198488.5: c.1309\_1311delinsTAA; p.(His437\*), was identified in both families. The disease-causing premature stop codon (TAA) had 2 sequence changes relative to the reference His<sup>437</sup> codon (CAC). The 2 variants probably did not occur simultaneously. The earlier variant, g.10595C>A; p.(His437Tyr), changed the CAC codon to CAA encoding Tyr<sup>437</sup>. This SNP (rs28573699) variant has an overall allele frequency of 0.06 in the gnomAD database. The resulting His-to-Tyr substitution is predicted to be benign according to PolyPhen-2 (Adzhubei et al. 2010). The more recent mutation (g.10593C>T) changed the existing CAA variant to TAA, a translation termination codon. This second change is a rare mutation, not listed in known genome databases.

### Family 3 (c.1375C>T; p.Gln459\*)

The proband of family 3, a 16-y-old Caucasian female from the United States, was a simplex case. All of her erupted permanent teeth have been restored, except for maxillary second molars, which showed evident enamel loss and tooth discoloration (Fig. 2). Radiographically, she had all permanent teeth except a canine (#11) and all first bicuspids, which had been extracted for orthodontic purposes. The enamel of developing third molars appeared hypoplastic over the occlusal surface and showed no contrast with dentin radiographically. Noticeably, the roots of most teeth looked long and thin. Dilaceration of root tips was evident on tooth numbers 3, 7, 8, 9, 10, 18, 24, and 31 (Fig. 2B). Exome analysis of the proband's DNA revealed a novel heterozygous nonsense mutation in *FAM83H* (NG\_016652.1: g.10659C>T; NM\_198488.5: c.1375C>T; p.Gln459\*). This mutation was not found in the proband's parents or the unaffected sibling and was a de novo mutation, as analysis of the whole exome

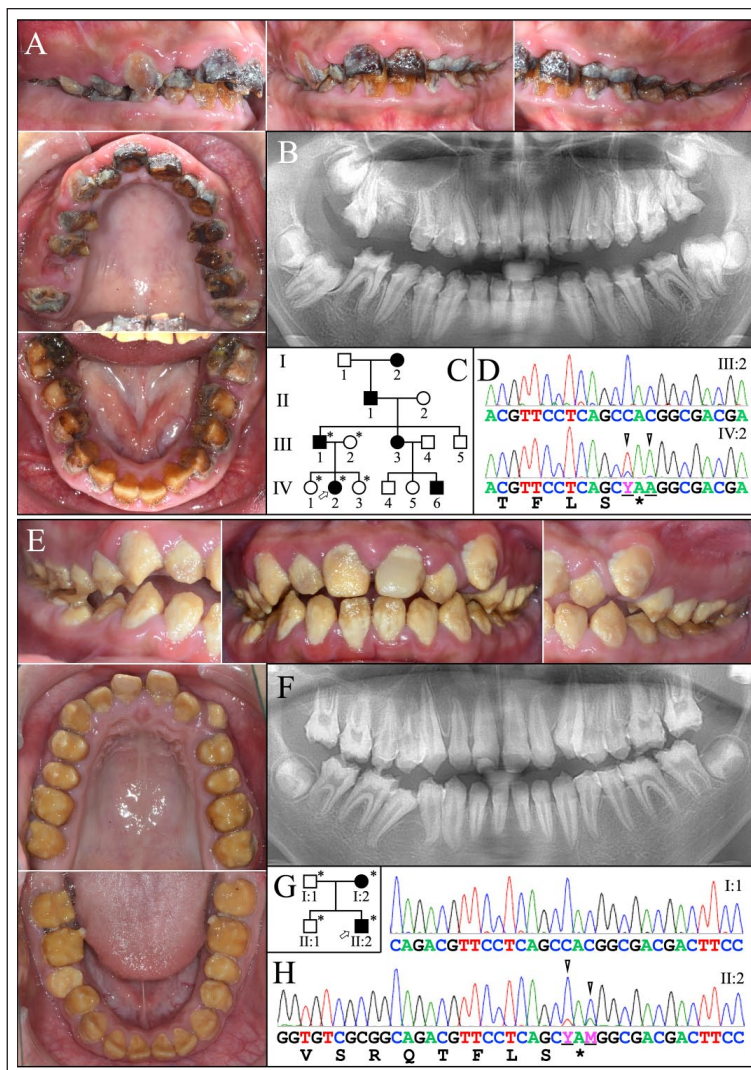


**Figure 1.** Families 1 and 2 from Taiwan with a novel *FAM83H* p.(His437\*) defect. (A–D) The family 1 proband (IV:2) at age 16 y presented with a darkly stained permanent dentition. Her panorex shows severe enamel attrition and failure of the mandibular second molars (#18 and #31) to erupt properly. The pedigree was consistent with a dominant pattern of inheritance. The DNA sequencing chromatogram shows the Y (C or T) and A variations (arrowheads) from the reference sequence that convert a CAC (histidine) codon into a TAA (stop) codon in 1 *FAM83H* allele. The conventional description for this mutation is as follows: NG\_016652.1: g.10593\_10595delinsTAA; NM\_198488.5: c.1309\_1311delinsTAA; p.(His437\*). (E–H) The family 2 proband (II:2) at age 13 y presented with a brown-stained permanent dentition with severe enamel attrition and failure of the right mandibular second bicuspid (#29) to erupt properly. The pedigree was consistent with a dominant pattern of inheritance. The DNA sequencing chromatogram shows the Y (C or T) and M (C or A) variations (arrowheads) from the reference sequence that introduce a TAA (stop) codon in 1 *FAM83H* allele.

sequences with InfiniumQCArray-24v1-0 confirmed paternity (Fig. 2C, D).

### Family 4 (c.1828G>T; p.Glu610\*)

Family 4 was a Taiwanese family showing an autosomal dominant pattern of inheritance for enamel defects (Fig. 3). The proband was diagnosed with AI in early childhood. According to



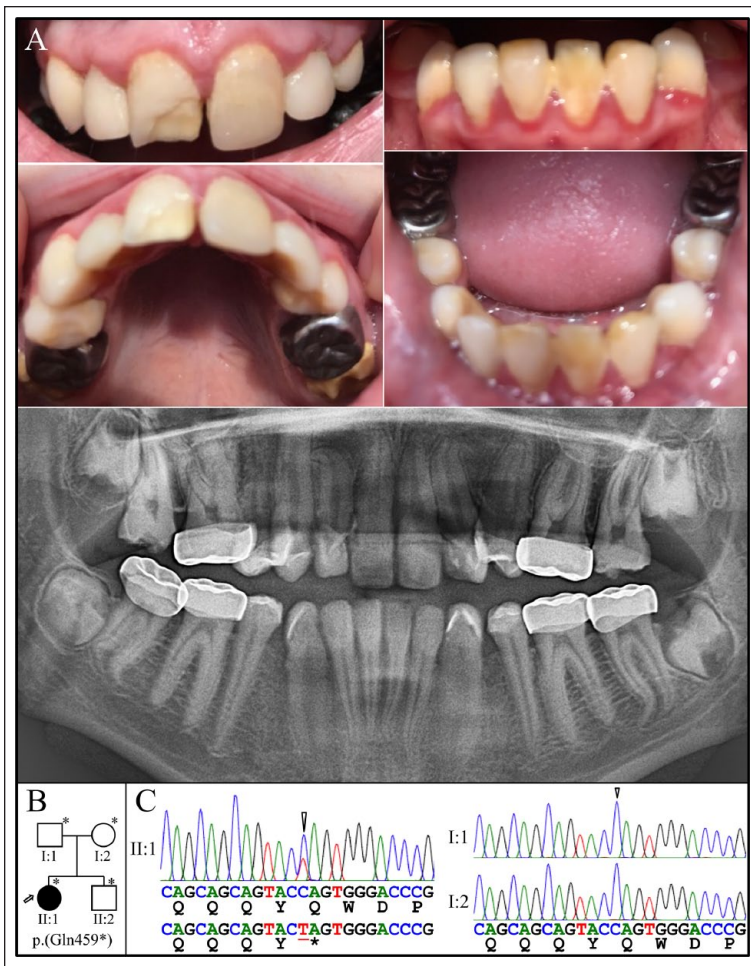


**Figure 2.** Family 3 from the United States with a novel *FAM83H* (p.Gln459\*) defect. (A) Dental phenotype of proband (II:1; age, 16 y). Radiographically there is little to no contrast between enamel and dentin in the unrestored maxillary second molars and unerupted third molars. The 4 first bicuspid and maxillary left canine (#11) had been extracted for orthodontic purposes. (B) The pedigree shows a simplex pattern. (C) The DNA sequencing chromatogram shows that the proband (II:1) was heterozygous for the *FAM83H* defect (left arrowhead). Neither parent held the defective *FAM83H* allele (right; arrowhead). The novel disease causing mutation is as follows: NG\_016652.1: g.10659C>T; NM\_198488.5: c.1375C>T; p.(Gln459\*).

his pediatric dentist, his permanent teeth had generally erupted on time but appeared rough upon emergence. The enamel was hypoplastic in many areas over the crown and was not particularly soft, giving the clinical impression of rough hypoplastic AI. At the time of recruitment, the proband (III:2; age, 13 y) had no retained primary teeth. All permanent teeth exhibited rough surfaces and acquired black stain. Most enamel appeared absent, with some remaining at the cusp tips of the canines, bicuspid, and molars, as well as their cervical areas. Radiographically, the erupted teeth showed no apparent enamel except for proximal areas of posterior teeth. Tooth numbers 2, 15, and 18 were vertically impacted with almost complete root formation and no apparent obstacles on the eruption path. The enamel of these unerupted teeth appeared ragged and hypoplastic at occlusal surfaces. These findings were consistently

observed from the serial orthopantomograms of the proband, indicating that the enamel roughness and thinness of unerupted teeth were not caused by pathologic resorption of the crown. This hypoplastic defect was particularly evident for the maxillary canines during development. Analysis of the proband's exome identified a novel G-to-T transversion in *FAM83H* (NG\_016652.1: g.11112G>T; NM\_198488.5: c.1828G>T) causing a premature termination codon (TAA) at position 610 (p.Glu610\*). No other disease-causing mutations in known AI candidate genes were detected.

### Families 5 to 9 with Known *FAM83H* Mutations

Four previously reported *FAM83H* mutations were identified in the following families: c.1330C>T (p.Gln444\*, family 5), c.1354C>T (p.Gln452\*, family 6), c.1408C>T (p.Gln470\*, family 8), and c.1915A>T (p.Lys639\*, family 7; Appendix Table). For the family 6 proband, the heterozygous *FAM83H* mutation was de novo, since neither of her parents carried this mutation.

The proband of family 5 was a 15-y-old male from Taiwan. Besides the obvious enamel hypocalcified defects, his dentition also showed generalized spacing and an anterior open bite (Appendix Fig. 1). Tooth number 11 was impacted without sufficient space for eruption. The enamel of this impacted tooth and developing third molars was of normal thickness but did not contrast with dentin. The family 6 proband was a 12-y-old Caucasian female from the United States who was apparently the only individual with hypocalcified AI. Her unrestored teeth exhibited the typical cheesy-soft appearance of ADHCAI (Appendix Fig. 2A–C). Family 7 from Taiwan had 3 persons diagnosed clinically with ADHCAI (Appendix Fig. 2D–E) but was not documented with oral photographs. However, the identified mutations segregated well with the reported enamel phenotypes.

Family 8 was a 3-generation Taiwanese family with 6 affected individuals (Appendix Figs. 3 and 4). The proband (III:3; age, 9 y) and his younger sister (III:4; age, 6 y) had mixed dentition, showing enamel defects on primary and permanent teeth. One of his cousins (III:2; age, 13 y) was also affected and had apparent impaction of tooth number 18. Family 9 was a previously recruited Hispanic family with ADHCAI (Kim et al. 2006), which was caused by the heterozygous *FAM83H* mutation: NG\_016652.1: g.10527G>T; NM\_198488.5: c.1243G>T; p.(Glu415\*) (Lee et al. 2008). Here we provide improved documentation of the proband's ADHCAI phenotype and, additionally, agenesis of 3 permanent first molars (#3, #14, #19; Appendix Fig. 5).

### Impacted Teeth in Cases with FAM83H Truncation Mutations

Noticing that several participants in our families had impacted teeth, including the probands of families 1, 4, and 5 and 1 affected individual (III:2) of family 8, we reviewed all previously reported ADHCAI cases with confirmed *FAM83H* disease-causing mutations. Only 2 of 19 studies that we searched mentioned the terms “impacted” or “impaction.” We then scrutinized the clinical radiographs for potential undocumented phenotypes and summarized the results in the Table. Among the 55 families from 19 studies, the probands of 4 families had or appeared to have at least 1 impacted tooth. The impactions involved canines, bicuspid, and second molars. The 4 families were of various ethnic backgrounds and carried different *FAM83H* truncation mutations: p.Arg325\* (Chinese), p.Glu383\* (Chinese), p.Gln452\* (Danish), and p.Gln677\* (Caucasian American).

### FAM83H and SEC16A Interaction

Given our previous interactome data of FAM83H, we identified another potential FAM83H-binding protein, SEC16A, which forms part of the COP II complex and mediates vesicle formation and protein transport from ER to Golgi. Pull-down assays were conducted to validate this interaction with different-length Flag-tagged FAM83Hs (WT, FAM83H<sup>287\*</sup>, and FAM83H<sup>697\*</sup>) and Halo-tagged SEC16A (Fig. 4). While full-length (WT) FAM83H and FAM83H<sup>697\*</sup> could pull down Halo-tagged SEC16A, FAM83H<sup>287\*</sup> could not, indicating that FAM83H interacted with SEC16A through its middle part (amino acids 287 to 697 of mouse FAM83H). No interaction between Flag-tagged full-length FAM83H and control HaloTag protein (~300 amino acids) validated the specificity of this interaction (Fig. 4B).

To test if a highly conserved sequence area of human FAM83H (664 to 688 amino acids) serves as an SEC16A binding site, we generated another construct, FAM83H<sup>657\*</sup>, to express a shorter form of truncated mouse FAM83H in which the conserved domain was deleted for pull-down assays. The results demonstrated that while FAM83H<sup>287\*</sup> did not show interaction with SEC16A, FAM83H<sup>657\*</sup> and FAM83H<sup>697\*</sup> could pull down Halo-tagged SEC16A, suggesting that amino acids 657 to 697 of mouse FAM83H (including the conserved domain) might not be critical for SEC16A binding.

### Discussion

Much evidence has indicated that the mutant truncated FAM83H protein with a length of 287 to 694 amino acids is essential for causing pathology in ameloblasts. Interestingly, within this disease-causing mutation region, there appears to be a gap between amino acids 470 and 610, where no truncation

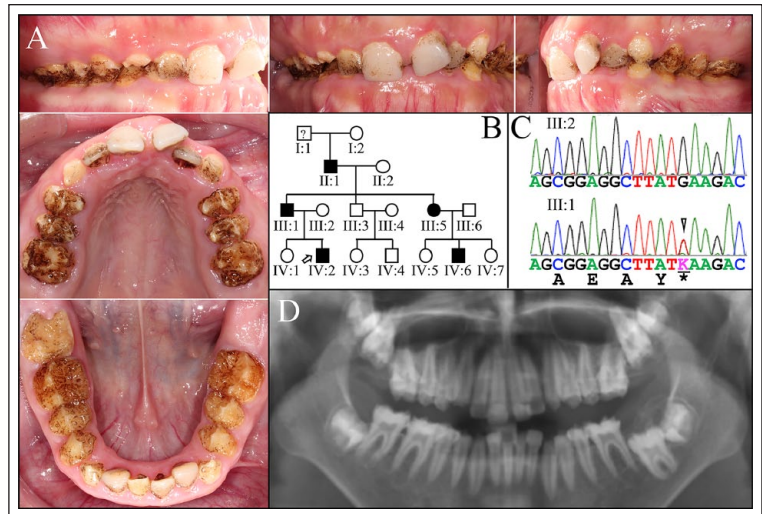


**Figure 3.** Family 4 from Taiwan with a novel *FAM83H* p.(Glu610\*) defect. **(A)** Dental phenotype of proband (III:2; age, 13 y) shows many stained pits on the surface of a hypoplastic enamel layer. **(B)** The pedigree is consistent with a dominant pattern of inheritance. **(C)** The DNA sequencing chromatogram shows a K (G or T) heterozygous variation (arrowhead) from the reference sequences that changes a GAA glutamate codon into a TAA (stop) codon in 1 *FAM83H* allele. This novel disease-causing mutation is as follows: NG\_016652.1: g.11112G>T; NM\_198488.5: c.1828G>T; p.(Glu610\*). **(D)** The panoramic radiograph shows vertically impacted second molars (#2, #15, and #18).

mutations have been reported. This specific distribution of causative mutations is puzzling. It seems unlikely that mutations in this gap will be identified as more families with ADHCAI are reported, since many mutations have been independently reported, some as many as 5 times in unrelated ADHCAI kindreds (Appendix Table). Seven mutations (p.Q452\*, p.Q456\*, p.Q457\*, p.Y458\*, p.Q459\*, p.W460\*, and p.Q463\*) cluster immediately before the N-terminal boundary (p.Q470\*) of the gap, supporting the noncoincidental nature of the gap. It may be that truncation mutations within this gap cause no enamel phenotype or a subtle one that is clinically difficult to identify. It has been recognized that the mRNA half-life and specific sequence motifs for RNA-binding proteins can modulate efficiency of nonsense-mediated decay (Lindeboom et al. 2016). Therefore, a premature termination codon within the gap region might cause instability of the transcript or trigger nonsense-mediated decay. Alternatively, a truncated FAM83H protein with a length of 470 to 610 amino acids, while being generated, might be somehow unstable and subject to protein degradation. For these hypothetical mechanisms, no or little mutant FAM83H protein will be present in ameloblasts; thus, amelogenesis is not disturbed. It has been proposed that the enamel defects of ADHCAI are caused by truncated FAM83H proteins that bind and mislocalize CK1 (Kuga, Kume, et al. 2016; Fulcher et al. 2018). Therefore, another possible explanation for the gap is that a FAM83H protein, when truncated between 470 and 610 amino acids, is unable to disrupt CK1 localization, which in turn cannot elicit

**Table.** Evidence for *FAM83H*-Associated Tooth Impaction.

| Reference: <i>FAM83H</i> Mutation | Impacted Teeth                                 | Ethnicity      | Search |
|-----------------------------------|--|----------------|--------|
| Lee et al. (2008)                 |  |                | No     |
| p.(Glu415*)                       | Not mentioned                                  | Hispanic       |        |
| p.(Tyr297*)                       | Not mentioned                                  | Asian          |        |
| p.(Trp460*)                       | Not mentioned                                  | Caucasian      |        |
| p.(Gln677*)                       | <b>Suspected impacted #15, #18, #31? (OPG)</b> | Caucasian      |        |
| Chan et al. (2011)                |  |                | No     |
| p.(Gln677*)                       | Not mentioned (3Y, too young)                  | Caucasian      |        |
| p.(Gln452*)                       | Not mentioned                                  | Caucasian      |        |
| Hyun et al. (2009)                |  |                | No     |
| p.(Gln452*)                       | Not mentioned (5Y8M, too young)                | Korean         |        |
| Haubek et al. (2011)              |  |                | Yes    |
| p.(Tyr302*)                       | Not mentioned                                  | Danish         |        |
| p.(Gln452*)                       | <b>Impacted canines and premolars</b>          | Danish         |        |
| Song et al. (2012)                |  |                | No     |
| p.(Tyr302*)                       | Not mentioned                                  | Chinese        |        |
| p.(Val309Rfs*16)                  | Not mentioned                                  | Chinese        |        |
| p.(Arg325*)                       | Not mentioned                                  | Chinese        |        |
| p.(Gln452*)                       | Not mentioned                                  | Chinese        |        |
| p.(Gln677*)                       | Not mentioned                                  | Chinese        |        |
| Wang et al. (2015)                |  |                | No     |
| p.(Gln452*)                       | Not mentioned                                  | Jewish         |        |
| p.(Gln457*)                       | No   | Turkish        |        |
| p.(Lys639*)                       | No   | Taiwanese      |        |
| Wright et al. (2009)              |  |                | No     |
| p.(Ser287*)                       | Not mentioned                                  | Caucasian      |        |
| p.(L308Rfs*16)                    | Not mentioned                                  | Caucasian      |        |
| p.(Trp460*)                       | Not mentioned                                  | Caucasian      |        |
| p.(Gln470*)                       | Not mentioned                                  | Caucasian      |        |
| p.(Gln470*)                       | Not mentioned                                  | Caucasian      |        |
| p.(Leu625Afs*79)                  | Not mentioned                                  | Caucasian      |        |
| p.(Glu694*)                       | Not mentioned                                  | Caucasian      |        |
| Xin et al. (2017)                 |  |                | Yes    |
| p.(Val311Rfs*14)                  | No   | Chinese        |        |
| p.(Arg325*)                       | <b>Suspected impacted #2, #15? (OPG)</b>       | Chinese        |        |
| p.(Ser377*)                       | Too young to determine                         | Chinese        |        |
| p.(Glu383*)                       | <b>Impacted #11</b>                            | Chinese        |        |
| Kim et al. (2008)                 |  |                | No     |
| p.(Arg325*)                       | Not mentioned                                  | Korean         |        |
| p.(Gln398*)                       | Not mentioned                                  | Korean         |        |
| Zhang et al. (2015)               |  |                | No     |
| p.(Arg325*)                       | No   | Chinese        |        |
| Hart et al. (2009)                |  |                | No     |
| p.(Gln398*)                       | Not mentioned                                  | Turkish        |        |
| p.(Gln444*)                       | Not mentioned                                  | Turkish        |        |
| p.(Gln456*) (5 families)          | Not mentioned                                  | Turkish        |        |
| p.(Gln456*) (de novo)             | Not mentioned                                  | Turkish        |        |
| Ding et al. (2009)                |  |                | No     |
| p.(Gln398*)                       | Too young to determine                         | Caucasian      |        |
| p.(Gln444*)                       | Too young to determine                         | Hispanic       |        |
| Wright et al. (2011)              |  |                | No     |
| p.(Gln398*) (2 families)          | Not mentioned                                  | No information |        |
| p.(Ser430*)                       | Not mentioned                                  | No information |        |
| p.(Gln677*) (2 families)          | Not mentioned                                  | No information |        |
| Yu et al. (2018)                  |  |                | No     |
| p.(Lys408*)                       | No   | Chinese        |        |
| Nowwarote et al. (2018)           |  |                | No     |
| p.(Glu421*)                       | No   | Thai           |        |
| Prasad et al. (2016)              |  |                | No     |
| p.(Gln428*)                       | Not mentioned                                  | No information |        |
| p.(Ser430*)                       | Not mentioned                                  | No information |        |
| p.(Gln677*)                       | Not mentioned                                  | No information |        |

(continued)



Table. (continued)

| Reference: <i>FAM83H</i> Mutation               | Impacted Teeth                                   | Ethnicity        | Search |
|---|--|------------------|--------|
| El-Sayed et al. (2010)<br>p.(Tyr458*)           | Not mentioned                                    | European         | No     |
| Kantaputra et al. (2016)<br>p.(Gln463*)         | No   | Thai             | No     |
| Lee et al. (2011)<br>p.(Gln665*)<br>p.(Gln677*) | Too young to determine<br>Too young to determine | Korean<br>Korean | No     |
| Current study<br>p.(His437*)                    | <b>Impacted #3 I</b>                             | Taiwanese        |        |
| p.(His437*)                                     | No   | Taiwanese        |        |
| p.(Gln459*)                                     | No   | USA              |        |
| p.(Glu610*)                                     | <b>Impacted #2, #15, #18</b>                     | Taiwanese        |        |
| p.(Gln444*)                                     | <b>Impacted #1 I</b>                             | Taiwanese        |        |
| p.(Gln452*) (de novo)                           | No   | No information   |        |
| p.(Gln470*)                                     | <b>Impacted #18 (affected cousin)</b>            | Taiwanese        |        |
| p.(Lys639*)                                     | No info  | Taiwanese        |        |
| p.(Glu415*)                                     | No info  | Hispanic         |        |

The dental phenotypes of all reported *FAM83H* defects causing autosomal dominant hypocalcified amelogenesis imperfecta were reviewed. Tooth impaction was never noted, except for 2 reports, and only rarely were radiographs provided that allowed it to be assessed retrospectively. However, the presence of impaction was sometimes found and should be assessed in future studies. OPG, panorex.

toxic effects in ameloblasts and cause little enamel malformation. Further investigations are warranted to test these hypotheses.

Unlike the typical phenotype of ADHCAI, the proband of family 4 in this study showed an evident hypoplastic component to his enamel defects, which partly resembled the enamel malformations of the *Fam83h* truncation mice that we recently characterized (Wang et al. 2019). In Witkop's (1957) original report of AI classification, it was stated that, for the hypocalcification type, "some degree of hypoplasia exists in this condition as the full thickness of the enamel is not formed on the occlusal one-half of the crown." This original characterization of patients with AI indicated that a localized hypoplastic defect could be found in some ADHCAI cases, which supported our findings from the family 4 proband. This phenotypic variation could be explained by the genotype. The novel nonsense mutation (p.Glu610\*) of family 4 reduces the size of the *FAM83H* mutation gap area mentioned earlier. Truncation mutations in this area could cause a more prominent hypoplastic component of enamel defects when compared with those outside this area. Alternatively, common sequence variants in genes related to enamel formation could serve as "genetic modifiers" and alter the enamel phenotype in ADHCAI. More cases have to be characterized and scrutinized to investigate the underlying mechanism of this phenotypic variation.

In this study, the probands of 3 families and an affected member of family 6 exhibited impacted teeth, which was not commonly reported for ADHCAI. These families are all from Taiwan, presumably of East or South Asian descent, suggesting that the genetic background might have a significant impact on the penetrance of altered tooth eruption in ADHCAI to which the genetic susceptibility is higher for Asian ethnicity. More interesting, the affected teeth are primarily canines and

second molars. While canine impaction is a common form of tooth impaction in the general population, impacted second molars are rare. The prevalence of impacted mandibular second molars was reported to be 0.65% in the Taiwanese population (Fu et al. 2012). The high frequency of second molar involvement suggested a distinct pathologic mechanism of altered tooth eruption in ADHCAI. We previously showed that *Fam83h* is expressed in ameloblasts and other enamel organ cells in developing mouse teeth. It is possible that mutant *FAM83H* proteins disturb cellular functions of enamel organ cells, composing part of dental follicle, for normal tooth eruption and cause impacted teeth in patients with ADHCAI. The high frequency of second molar impaction might plausibly result from its later timing and longer duration of tooth development, which predisposes enamel organ cells to pathology caused by mutant *FAM83H* proteins.

We here demonstrate that *FAM83H* interacts with SEC16A, a protein component of the COP II complex critical for ER-to-Golgi transport. This finding suggested that *FAM83H* might bring CK1 to the ER exit site to facilitate vesicle trafficking between ER and Golgi. Structural analyses of the COPII vesicle coat have shown that SEC16 and SEC13 form a 2:2 tetramer that serves as a template for coat assembly (Whittle and Schwartz 2010). The tetramer is arranged such that 2 SEC16 molecules homodimerize in the center of an elongated structure of which SEC13 forms the 2 ends. We previously demonstrated that *FAM83H* might form a homodimer (Wang et al. 2015), which is consistent with that of SEC16 in the SEC13-SEC16 edge element and supports our hypothesis that *FAM83H* might function in ER-to-Golgi membrane trafficking (Ding et al. 2009). While this potential role of *FAM83H* on protein secretion seems to explain the hypoplastic component of enamel phenotypes found in *Fam83h* truncation mice and

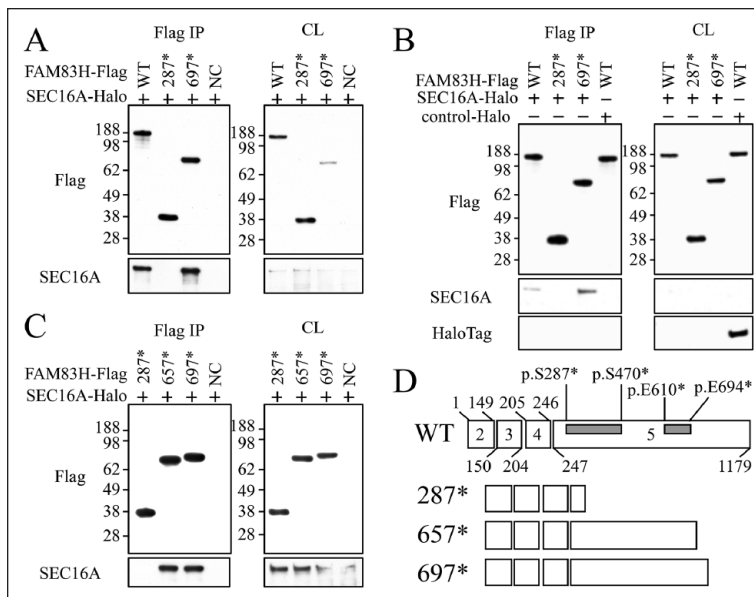


**Figure 4.** FAM83H-SEC16A interaction. **(A)** Pull-down assay of C-terminal truncated mouse FAM83H proteins (numbers are homologous to human pathogenic variants). Halo-tagged SEC16A and I of the Flag-tagged FAM83H proteins with various length (WT, full length; 287\*, amino acids 1 to 287; 697\*, amino acids 1 to 697; -, Flag tag only) were expressed and  $\alpha$ -Flag immunoprecipitated. The IP products as well as initial cell lysates (CL) were blotted with  $\alpha$ -Flag (top) and  $\alpha$ -HaloTag (bottom) antibodies. While full-length FAM83H and FAM83H<sup>697\*</sup> (Flag tagged) can pull down SEC16A (Halo tagged), FAM83H<sup>287\*</sup> cannot, suggesting that the middle part of FAM83H (amino acids 287 to 697) may be responsible for interacting with SEC16A. Bands of ~140, ~36, and ~75 kDa are full-length FAM83H, FAM83H<sup>287\*</sup>, and FAM83H<sup>697\*</sup>, respectively. **(B)** Pull-down assay of FAM83H and control HaloTag protein. Similar pull-down assays were performed with control HaloTag protein (HaloTag is ~300 amino acids long). Full-length FAM83H (Flag tagged) can pull down SEC16A (Halo tagged) but not HaloTag protein, demonstrating the specificity of FAM83H-SEC16A interaction; the interaction is not through HaloTag. Top: Bands of ~140, ~36, and ~75 kDa are full-length FAM83H, FAM83H<sup>287\*</sup>, and FAM83H<sup>697\*</sup>, respectively. Bottom: SEC16A-Halo is ~270 kDa, and control HaloTag protein is ~30 kDa. **(C)** Pull-down assay of FAM83H<sup>657\*</sup>. Similar pull-down assays were performed with another C-terminal truncated FAM83H (657\*, amino acids 1 to 657). FAM83H<sup>657\*</sup> and FAM83H<sup>697\*</sup> (Flag tagged) can pull down SEC16A (Halo tagged), suggesting that the region between amino acid 657 and 697 may not be necessary for FAM83H-SEC16A interaction. The ~70-kDa band is FAM83H<sup>657\*</sup>. **(D)** Top: Human FAM83H gene shows the amino acid encoded on exons 2 to 5 and the range of human FAM83H pathogenic variants that cause autosomal dominant hypocalcified amelogenesis imperfecta. Bottom: Truncated recombinant mouse proteins analogous to human pathogenic variants used in this study.

some patients with ADHCAI, simple loss of FAM83H-SEC16A interaction is not a plausible mechanism of the enamel defects, as *Fam83h*-null mice exhibit no overall enamel malformations, including hypoplasia. In other words, the toxic effects on ameloblasts from mutant FAM83H proteins are the cause of enamel defects, not the loss of any FAM83H functions, including the FAM83H-SEC16A interaction reported here. Nevertheless, this interaction may be critical for FAM83H functions outside of amelogenesis, which requires further investigation.

### Author Contributions

S.K. Wang, contributed to conception, design, data acquisition, analysis, and interpretation, drafted and critically revised the manuscript; H. Zhang, C.Y. Hu, J.F. Liu, S. Chadha, contributed to

conception and data acquisition, critically revised the manuscript; J.W. Kim, contributed to conception, data acquisition, and analysis, critically revised the manuscript; J.P. Simmer, contributed to conception, design, data acquisition, and analysis, drafted and critically revised the manuscript; J.C.C. Hu, contributed to conception, design, data acquisition, analysis, and interpretation, critically revised the manuscript. All authors gave final approval and agree to be accountable for all aspects of the work.

### Acknowledgments

We thank the families for their participation in this study.

### Declaration of Conflicting Interests

The authors declared no potential conflicts of interest with respect to the research, authorship, and/or publication of this article.

### Funding

The authors disclosed receipt of the following financial support for the research, authorship, and/or publication of this article: This study was supported by the National Institutes of Health (grants DE015846 to J.C.C.H. and DE027675 to J.P.S.), Ministry of Science and Technology in Taiwan (grant 108-2314-B-002-038-MY3 to S.K.W.), and National Taiwan University Hospital (grant 107-N3966 to S.K.W.).

### ORCID iDs

J.W. Kim <https://orcid.org/0000-0002-9399-2197>  
J.P. Simmer <https://orcid.org/0000-0002-7192-6105>

### Data Availability Statement

Whole exome sequencing data and analysis are available at dbGaP under Genetics of Disorders Affecting Tooth Structure, Number, Morphology and Eruption. dbGaP study accession: phs001491.

v1.p1. Additional data used to support the findings of this study are available from the corresponding author upon request.

### References

- Azhubei IA, Schmidt S, Peshkin L, Ramensky VE, Gerasimova A, Bork P, Kondrashov AS, Sunyaev SR. 2010. A method and server for predicting damaging missense mutations. *Nat Methods*. 7(4):248–249.
- Blackburn JB, D'Souza Z, Lupashin VV. 2019. Maintaining order: COG complex controls Golgi trafficking, processing, and sorting. *FEBS Lett*. 593(17):2466–2487.
- Chan HC, Estrella NM, Milkovich RN, Kim JW, Simmer JP, Hu JC. 2011. Target gene analyses of 39 amelogenesis imperfecta kindreds. *Eur J Oral Sci*. 119 Suppl 1:311–323.
- Ding Y, Estrella MR, Hu YY, Chan HL, Zhang HD, Kim JW, Simmer JP, Hu JC. 2009. Fam83H is associated with intracellular vesicles and ADHCAI. *J Dent Res*. 88(11):991–996.
- Duden R. 2003. ER-to-Golgi transport: COP I and COP II function (review). *Mol Membr Biol*. 20(3):197–207.



- El-Sayed W, Shore RC, Parry DA, Inglehearn CF, Mighell AJ. 2010. Ultrastructural analyses of deciduous teeth affected by hypocalcified amelogenesis imperfecta from a family with a novel Y458X FAM83H nonsense mutation. *Cells Tissues Organs*. 191(3):235–239.
- Fu PS, Wang JC, Wu YM, Huang TK, Chen WC, Tseng YC, Tseng CH, Hung CC. 2012. Impacted mandibular second molars. *Angle Orthod*. 82(4):670–675.
- Fulcher LJ, Bozatz P, Tachie-Menson T, Wu KZL, Cummins TD, Bufton JC, Pinkas DM, Dunbar K, Shrestha S, Wood NT, et al. 2018. The DUF1669 domain of FAM83 family proteins anchor casein kinase 1 isoforms. *Sci Signal*. 11(531):eaao2341.
- Hart PS, Becerik S, Cogulu D, Emingil G, Ozdemir-Ozenen D, Han ST, Sulima PP, Firatli E, Hart TC. 2009. Novel FAM83H mutations in Turkish families with autosomal dominant hypocalcified amelogenesis imperfecta. *Clin Genet*. 75(4):401–404.
- Haubek D, Gjørup H, Jensen LG, Juncker I, Nyegaard M, Borglum AD, Poulsen S, Hertz JM. 2011. Limited phenotypic variation of hypocalcified amelogenesis imperfecta in a Danish five-generation family with a novel FAM83H nonsense mutation. *Int J Paediatr Dent*. 21(6):407–412.
- Hu JC, Chun YH, Al Hazzazzi T, Simmer JP. 2007. Enamel formation and amelogenesis imperfecta. *Cells Tissues Organs*. 186(1):78–85.
- Hyun HK, Lee SK, Lee KE, Kang HY, Kim EJ, Choung PH, Kim JW. 2009. Identification of a novel FAM83H mutation and microhardness of an affected molar. *Int Endod J*. 42(11):1039–1043.
- Kantaputra PN, Intachai W, Auychai P. 2016. All enamel is not created equal: supports from a novel FAM83H mutation. *Am J Med Genet A*. 170A(1):273–276.
- Kim JW, Lee SK, Lee ZH, Park JC, Lee KE, Lee MH, Park JT, Seo BM, Hu JC, Simmer JP. 2008. FAM83H mutations in families with autosomal-dominant hypocalcified amelogenesis imperfecta. *Am J Hum Genet*. 82(2):489–494.
- Kim JW, Simmer JP, Lin BP, Seymen F, Bartlett JD, Hu JC. 2006. Mutational analysis of candidate genes in 24 amelogenesis imperfecta families. *Eur J Oral Sci*. 114 Suppl 1:3–12.
- Kim JW, Zhang H, Seymen F, Koruyucu M, Hu Y, Kang J, Kim YJ, Ikeda A, Kasimoglu Y, Bayram M, et al. 2019. Mutations in RELT cause autosomal recessive amelogenesis imperfecta. *Clin Genet*. 95(3):375–383.
- Kuga T, Kume H, Adachi J, Kawasaki N, Shimizu M, Hoshino I, Matsubara H, Saito Y, Nakayama Y, Tomonaga T. 2016. Casein kinase 1 is recruited to nuclear speckles by FAM83H and SON. *Sci Rep*. 6:34472.
- Kuga T, Kume H, Kawasaki N, Sato M, Adachi J, Shiromizu T, Hoshino I, Nishimori T, Matsubara H, Tomonaga T. 2013. A novel mechanism of keratin cytoskeleton organization through casein kinase 1 $\alpha$  and FAM83H in colorectal cancer. *J Cell Sci*. 126(Pt 20):4721–4731.
- Kuga T, Sasaki M, Mikami T, Miake Y, Adachi J, Shimizu M, Saito Y, Koura M, Takeda Y, Matsuda J, et al. 2016. FAM83H and casein kinase I regulate the organization of the keratin cytoskeleton and formation of desmosomes. *Sci Rep*. 6:26557.
- Lee SK, Hu JC, Bartlett JD, Lee KE, Lin BP, Simmer JP, Kim JW. 2008. Mutational spectrum of FAM83H: the C-terminal portion is required for tooth enamel calcification. *Hum Mutat*. 29:E95–E99.
- Lee SK, Lee KE, Jeong TS, Hwang YH, Kim S, Hu JC, Simmer JP, Kim JW. 2011. FAM83H mutations cause ADHCAI and alter intracellular protein localization. *J Dent Res*. 90(3):377–381.
- Lindeboom RG, Supek F, Lehner B. 2016. The rules and impact of nonsense-mediated mRNA decay in human cancers. *Nat Genet*. 48(10):1112–1118.
- Nowwarote N, Theerapanon T, Osathanon T, Pavasant P, Porntaveetus T, Shotelersuk V. 2018. Amelogenesis imperfecta: a novel FAM83H mutation and characteristics of periodontal ligament cells. *Oral Dis*. 27(10):12926.
- Prasad MK, Geoffroy V, Vicaire S, Jost B, Dumas M, Le Gras S, Switala M, Gasse B, Laugel-Haushalter V, Paschaki M, et al. 2016. A targeted next-generation sequencing assay for the molecular diagnosis of genetic disorders with orofacial involvement. *J Med Genet*. 53(2):98–110.
- Song YL, Wang CN, Zhang CZ, Yang K, Bian Z. 2012. Molecular characterization of amelogenesis imperfecta in chinese patients. *Cells Tissues Organs*. 196(3):271–279.
- Wang SK, Hu Y, Smith CE, Yang J, Zeng C, Kim JW, Hu JC, Simmer JP. 2019. The enamel phenotype in homozygous FAM83H truncation mice. *Mol Genet Genomic Med*. 7(6):e724.
- Wang SK, Hu Y, Yang J, Smith CE, Richardson AS, Yamakoshi Y, Lee Y-L, Seymen F, Koruyucu M, Gencay K, et al. 2015. FAM83H null mice support a neomorphic mechanism for human ADHCAI. *Mol Genet Genomic Med*. 4(1):46–67.
- Whittle JR, Schwartz TU. 2010. Structure of the Sec13-Sec16 edge element, a template for assembly of the COPII vesicle coat. *J Cell Biol*. 190(3):347–361.
- Witkop CJ. 1957. Hereditary defects in enamel and dentin. *Acta Genet Stat Med*. 7(1):236–239.
- Witkop CJ Jr. 1988. Amelogenesis imperfecta, dentinogenesis imperfecta and dentin dysplasia revisited: problems in classification. *J Oral Pathol*. 17(9–10):547–553.
- Witkop CJ Jr, Sauk JJ Jr. 1976. Heritable defects of enamel. In: Stewart RE, Prescott GH, editors. *Oral facial genetics*. St. Louis (MO): C.V. Mosby Co. p. 151–226.
- Wright JT, Frazier-Bowers S, Simmons D, Alexander K, Crawford P, Han ST, Hart PS, Hart TC. 2009. Phenotypic variation in FAM83H-associated amelogenesis imperfecta. *J Dent Res*. 88(4):356–360.
- Wright JT, Torain M, Long K, Seow K, Crawford P, Aldred MJ, Hart PS, Hart TC. 2011. Amelogenesis imperfecta: genotype-phenotype studies in 71 families. *Cells Tissues Organs*. 194(2–4):279–283.
- Xin W, Wenjun W, Man Q, Yuming Z. 2017. Novel FAM83H mutations in patients with amelogenesis imperfecta. *Sci Rep*. 7(1):6075.
- Yu S, Quan J, Wang X, Sun X, Zhang X, Liu Y, Zhang C, Zheng S. 2018. A novel FAM83H mutation in one Chinese family with autosomal-dominant hypocalcification amelogenesis imperfecta. *Mutagenesis*. 33(4):333–340.
- Zhang C, Song Y, Bian Z. 2015. Ultrastructural analysis of the teeth affected by amelogenesis imperfecta. *Oral Surg Oral Med Oral Pathol Oral Radiol*. 119(2):e69–e76.
- Zhang H, Hu Y, Seymen F, Koruyucu M, Kasimoglu Y, Wang SK, Wright JT, Havel MW, Zhang C, Kim JW, et al. 2019. Enam mutations and digenic inheritance. *Mol Genet Genomic Med*. 7(10):e00928.